Proceedings of ALGORITMY 2005
pp. 185–193

# MICRO AND MACRO LEVEL STOCHASTIC SIMULATION OF REACTION-DIFFUSION SYSTEMS *

ISTVÁN LAGZI† AND FERENC IZSÁK‡

**Abstract.** We provide numerical simulations for nonlinear reaction-diffusion systems, which arise from a micro and macro level model of pattern formation (Liesegang phenomenon). In both cases we apply a stochastic approach: a discrete stochastic model and concentration perturbation in a deterministic model.

**Key words.** reaction-diffusion systems, pattern formation, Liesegang phenomenon, stochastic models, numerical simulations

**AMS subject classifications.** 35K57, 35K60, 37M05

## 1. Introduction.

**1.1. Liesegang phenomenon.** In reaction-diffusion systems pattern formation generally occurs due to the interaction of diffusion process with nonlinear chemical reaction. Liesegang presented the first experimental evidence of such patterns [1]. In this case the pattern is the distribution of the product (precipitate) in a chemical reaction. In the experimental setup we take two initially separated electrolytes (ionic species), one of them (inner electrolyte) is uniformly distributed in a gel (diffusion column) and the other one (outer electrolyte) diffuses from outside into the diffusion column. A well-detectable pattern structure evolves in several days. In a $1D$ or quasi-$1D$ case (planar reaction front) one can observe disjoint parallel zones of precipitate. An electric field highly influences the evolution of the patterns due to the ionic migration.
The detailed investigations on Liesegang phenomenon have showed four empirical regularities, between the following (positive real) macroscopic quantities: the position $X_n$ of the $n$th precipitation zone measured from the junction point of electrolytes ,the width $w_n$ of the $n$th band, and the time $\tau_n$ elapsed until its formation.
The spacing law states that the positions of precipitate form an asymptotically geometric series:

$$\lim_{n\to\infty} X_{n+1}/X_n = 1 + p,$$

where $1 + p$ is the spacing coefficient. According to the time law for Liesegang patterning, these two quantities always correspond to the following relation:

$$X_n = a_1 \tau_n^{1/2} + c_1$$

[10], with $a_1, c_1 \in \mathbf{R}^+$ are constants depending on experimental conditions. The width law describes the dependence of the thickness of zones on their position [4]:

$$w_n = c_2 X_n^{\alpha},$$

*This work was supported by Grant No.: D048673 (OTKA) and 00585/2003 (OMFB, IKTA5-137).

†Department of Physical Chemistry, Eötvös University, 1117 Pázmány Péter sétány 1/A., Budapest, Hungary, +361209-0555 (lagzi@vuk.chem.elte.hu).

‡Department of Applied Analysis, Eötvös University, 1117 Pázmány Péter sétány 1/C., Budapest, Hungary, +361209-0555 (izsakf@cs.elte.hu).

where $c_2$ and $\alpha$ are constants. Real experiments and some theoretical studies suggest that $\alpha = 1$. Finally, the Matalon–Packter law shows the influence of the initial concentration $a_0$ and $b_0$ of the electrolytes on spacing coefficient:

$$p = F(b_0) + \frac{1}{a_0} G(b_0),$$

with $F$ and $G$ real functions [3], which can be specified in some situations.

Kai *et al.* [5] presented that low initial concentration difference ($\Delta = a_0 - b_0$) (in the absence of an electric field) leads to considerable uncertainty (weak reproducibility of the band locations and of the band formation), in terms of the location of bands and of the appearance time. Experimental investigations have shown that pattern formation exhibits increasingly stochastic behavior (in the above sense) as $\Delta$ approaches zero.

Earlier, when the cited experiments were performed the detailed simulation of stochastic pattern formation was not possible due to the limited computational resources. In the present study we will confirm the experimental findings and predict the behavior of the system in case of coupling the diffusion and ionic migration transport (pattern formation in the presence of an electric field).

**1.2. Chemical scheme.** Our chemical mechanism describing the precipitate formation contains one single step. The outer electrolyte ($A^+$) and the inner electrolyte ($B^-$) form directly the precipitate ($P$) as: $A^+ + B^- \longrightarrow P$.

**1.3. Governing equations in the deterministic case.** Evolution of precipitation patterns in $1D$ can be described by the following reaction-diffusion equations – all quantities are dimensionless:

$$\begin{aligned} \frac{\partial a}{\partial \tau} &= D_a \frac{\partial^2 a}{\partial x^2} - z_a \epsilon \frac{\partial a}{\partial x} - \delta(P,K,L), \\ \frac{\partial b}{\partial \tau} &= D_b \frac{\partial^2 b}{\partial x^2} - z_b \epsilon \frac{\partial b}{\partial x} - \delta(P,K,L), \\ \frac{\partial p}{\partial \tau} &= \delta(P,K,L), \end{aligned} \tag{1.1}$$

where $a, b$ and $p : [0,T] \times [0,l] \to \mathbf{R}$ yield the concentrations of the outer and the inner electrolyte and the amount of the precipitate. $D_a, D_b \in \mathbf{R}^+$ denote the diffusion coefficients, $z_a, z_b \in \mathbf{Z}$ are related to the charges of the electrolytes, while $\epsilon$ is the yields dimensionless electric field strength, which incorporates the mobility of the ions. The initial and boundary conditions will be specified later. For a detailed discussion of the model and deterministic simulation results we refer to [8] and for an alternative model to [2]. Since the precipitate does not diffuse, the diffusion term for the precipitate has been eliminated. Finally, the reaction term $\delta(P,K,L) : [0,T] \times [0,l] \to \mathbf{R}$ is defined as follows:

if $p = 0$ (there is no precipitate), then

$$\delta(P,K,L) = \kappa S_P \Theta(P - K), \tag{1.2}$$

if $p > 0$ (there is some precipitate), then

$$\delta(P,K,L) = \kappa S_P \Theta(P - L), \tag{1.3}$$

where $\kappa \in \mathbf{R}^+$ is the rate constant of the precipitation reaction, $L \in \mathbf{R}^+$ is the solubility product, $K \in \mathbf{R}^+$ is the nucleation product and $\Theta : \mathbf{R} \to \mathbf{R}$ is the Heaviside

step function. $S_P$ yields the amount of the precipitate which can form, defined as follows (based on Ostwald's supersaturation model proposed by Büki et al. [8], [9]):

$$S_P = \frac{1}{2}\left[(a+b) - \sqrt{(a+b)^2 - 4(P-L)}\right]. \tag{1.4}$$

The basis of the model is that precipitation occurs only if the product of the concentrations reaches $K$. However, if previously formed precipitate is present, it promotes the precipitation process and the product of the concentrations has to reach only a lower threshold $L$.

## 2. Models.

**2.1. Stochastic perturbation in the deterministic model - macro level approach.** We apply perturbation for the concentrations of the electrolytes in (1.1) in order to take into account the inherent fluctuations of the system [7]. We suppose that the concentration of both electrolytes consists of two parts:

$$a = \bar{a} + a' \quad \text{and} \quad b = \bar{b} + b', \tag{2.1}$$

where $\bar{a}, \bar{b} : [0,T] \times [0,l] \to \mathbf{R}$ are the average concentrations (expected values), while $a', b' : [0,T] \times [0,l] \to \mathbf{R}$ yield the concentration fluctuations. Variations of fluctuations $\frac{\partial a'}{\partial \tau}$ and $\frac{\partial b'}{\partial \tau}$ are usually considered to be zero when applying a time discretization in the simulations since the average effect of these terms over any time interval is zero. Inserting (2.1) into (1.1) gives

$$\begin{aligned}
\frac{\partial \bar{a}}{\partial \tau} &= D_a \frac{\partial^2(\bar{a}+a')}{\partial x^2} - z_a \epsilon \frac{\partial(\bar{a}+a')}{\partial x} - \delta((\bar{a}+a')(\bar{b}+b'), K, L), \\
\frac{\partial \bar{b}}{\partial \tau} &= D_b \frac{\partial^2(\bar{b}+b')}{\partial x^2} - z_b \epsilon \frac{\partial(\bar{b}+b')}{\partial x} - \delta((\bar{a}+a')(\bar{b}+b'), K, L), \\
\frac{\partial p}{\partial \tau} &= \delta((\bar{a}+a')(\bar{b}+b'), K, L).
\end{aligned} \tag{2.2}$$

During the computation process, first the concentration of the two electrolytes were perturbed, then the diffusion and the reaction terms were consecutively calculated with the perturbed concentrations. This process has been repeated in every time step. Perturbation $a'$ of $\bar{a}$ (or perturbation $b'$ of $\bar{b}$) can be described as the summed up random effects acting on each particles (of type $A$ or $B$). At the microscopic level the only assumption was that the displacement of all particles are identically distributed. The mean of this distribution is related to the electric field strength ($\epsilon$), while its variance is proportional to the fluctuations in the system.
Application of the central limit theorem gives that the change of concentration (which can be described by the displacement of particles) is normally distributed: the mean is determined again by $\epsilon$, while its standard deviation is proportional to the square root of the number of ions, i.e. that of the concentration. Therefore, the perturbations of the concentrations were calculated as follows:

$$\begin{aligned}
a' &= \texttt{rand}(x,\tau) d \sqrt{\bar{a}}, \\
b' &= \texttt{rand}(x,\tau) d \sqrt{\bar{b}},
\end{aligned}$$

where $d$ is related to the magnitude of the fluctuations and $\texttt{rand}(x,\tau)$ is a normally distributed random number. It has been generated for the different electrolytes in

every position in each time step.
System (2.2) has been solved numerically using a "method of lines" technique. We can reduce (2.2) to a set of ordinary differential equations after spatial discretization (finite difference) on an equidistant $1D$ spatial grid. The produced ordinary differential equations have been integrated in time using a second order Runge–Kutta method with the following boundary conditions:

$$a|_{x=0} = a_0, \quad \left.\frac{\partial b}{\partial x}\right|_{x=0} = \left.\frac{\partial a}{\partial x}\right|_{x=l} = \left.\frac{\partial b}{\partial x}\right|_{x=l} = 0,$$

where $l$ is the length of the diffusion column. In all simulations we used the parameter set $D_a = D_b = 0.4,\ K = 0.13,\ L = 0.1,\ \kappa = 250, z_a = 1, z_b = -1,\ l = 480$ and $d = 0.0003$. The initial conditions were

$$a(0,x) = a_0\Theta(-x),\ b(0,x) = b_0\Theta(x) \quad \text{and} \quad p(0,x) = 0.$$

The grid spacing was $\Delta x = 0.4$ and we performed numerical simulations with the time step $\Delta\tau = 0.004$.

**2.2. Discrete stochastic model - micro level approach.** A micro level (discrete) stochastic model for chemical reactions [11] is more realistic in the sense that the system is described using finite number of particles [6]. Accordingly we assume three types of particles: $A$ and $B$ for the reactants and $P$ for the precipitate. We also apply a spatial discretization: the reaction space is splitted into $I$ small "segments" (the distance of their midpoint is 1) such that the whole system is described with the number of each particles in the segments. Formally, we give it with a state vector at (time) $t$: $(M_A(t); M_B(t); M_P(t)) \in (\mathbf{N}^I \times \mathbf{N}^I \times \mathbf{N}^I)$, where $M_A[i](t)$ gives the number of the $A$ type particles in the $i$th segment at time $t$. Our aim is to model the evolution of the process during a (short) time interval $(t, t+h)$, i.e. we try to find a time step operator $F_h$ such that $F_h(M_A(t); M_B(t); M_P(t)) = (M_A(t+h); M_B(t+h); M_P(t+h))$. Henceforth we consider the state vector at a given time $t$ and investigate the time step.
In the discrete model displacements of particles of length less than 0.5 correspond to " step = 0 ", that is, in the model they will rest in their position. Similarly, particles with displacements between -0.5 and -1.5 are mapped to the segment to the left from the actual one (" step = -1 "), while those between +0.5 and +1.5 will move to the right of the actual position. In our model we have allowed five steps: -2, -1, 0, 1, 2. Displacements of particles $A$ and $B$ in electric field free case and without reaction terms could be modeled using a discretized version of Brownian motion. This means that for the transition probabilities in this limited case we obtain

$$p_2 = P(\text{step} = 2) = p_{-2} = P(\text{step} = -2) = \int_{-\infty}^{-1.5} \Phi(x)\,\mathrm{d}x \approx 0.0668,$$

$$p_1 = P(\text{step} = 1) = p_{-1} = P(\text{step} = -1) = \int_{-1.5}^{-0.5} \Phi(x)\,\mathrm{d}x \approx 0.2417$$

and

$$p_0 = P(\text{step} = 0) = \int_{-0.5}^{0.5} \Phi(x)\,\mathrm{d}x \approx 0.383,$$

where $\Phi$ denotes the density function of the standard normal distribution. In the model one may suppose that the homogeneous electric field modifies only the transport of the electrolyte coming from outside, i.e. we have to change only the transition probabilities of particles $A$. If the electric field promotes the motion of the reaction front (" positive field ") we push every particle $A$ to the right with probability $\epsilon_+$ and leave it in its original position with probability $1-\epsilon_+$, where $0 \leq \epsilon_+ \leq 1$ is related to the electric field strength. Therefore, the transition probabilities $P_{\epsilon_+}$ (according to the external electric field) of particles $A$ are given as follows:

$$P_{\epsilon_+}(\text{step}=1) = P(\text{step}=0)\epsilon_+ + P(\text{step}=1)(1-\epsilon_+) = p_0\epsilon_+ + p_1(1-\epsilon_+),$$

$$P_{\epsilon_+}(\text{step}=0) = p_{-1}\epsilon_+ + p_0(1-\epsilon_+), \quad P_{\epsilon_+}(\text{step}=-1) = p_{-2}\epsilon_+ + p_{-1}(1-\epsilon_+),$$

$$P_{\epsilon_+}(\text{step}=-2) = p_{-2}(1-\epsilon_+), \quad P_{\epsilon_+}(\text{step}=2) = p_1\epsilon_+ + p_2.$$

Similarly, if the electric field retards the diffusion of the outer electrolyte $A$ (" negative field "), we modify the transition probabilities as follows:

$$P_{\epsilon_-}(\text{step}=1) = p_2\epsilon_- + p_1(1-\epsilon_-), \quad P_{\epsilon_-}(\text{step}=0) = p_{-1}\epsilon_- + p_0(1-\epsilon_-),$$

$$P_{\epsilon_-}(\text{step}=-1) = p_0\epsilon_- + p_{-1}(1-\epsilon_-), \quad P_{\epsilon_-}(\text{step}=-2) = p_{-1}\epsilon_- + p_{-2},$$

$$P_{\epsilon_-}(\text{step}=2) = p_2(1-\epsilon_-),$$

where $0 \leq \epsilon_- \leq 1$ again characterizes the electric field strength.
The precipitation reaction was modeled by Ostwald's supersaturation theory [10] the basic idea of which is that precipitation can take place only if the local concentration product of the electrolytes reaches a certain threshold (nucleation product). At the same time the reaction promotes the further process and the mentioned threshold value falls back in this case.
During the calculation of the actual particle numbers we have to take into account all the particles, that reside or go through a given segment (as a potential reagent). These summed up particle numbers are denoted by $\text{SUM}_A[i](t)$ and $\text{SUM}_B[i](t)$. This generalization of the " point concentrations " makes possible to take into account some stochastic effects. In the simulations we calculated the reaction term by the following algorithm. If $M_P[i](t) = 0$ (there is no precipitate at the $i$th segment), a deterministic approach would result in the following amount of precipitated material, similarly to (1.2):

$$\Delta[i](t) = \sigma[i](t)\Theta(\text{SUM}_A[i](t)\text{SUM}_A[i](t) - K)$$

and for the case when $M_P[i](t) \neq 0$ we substitute $K \in \mathbf{N}$ (corresponding to the nucleation product) with $L \in \mathbf{N}$, which is related to the solubility product in (1.3). Here $\sigma[i](t)$ is given as follows according to (1.4):

$$\sigma[i](t) = \frac{1}{2}\left(\text{SUM}_A[i](t) + \text{SUM}_B[i](t) - \sqrt{(\text{SUM}_A[i](t) + \text{SUM}_B[i](t))^2 - 4(\text{SUM}_A[i](t)\text{SUM}_B[i](t) - L)}\right).$$

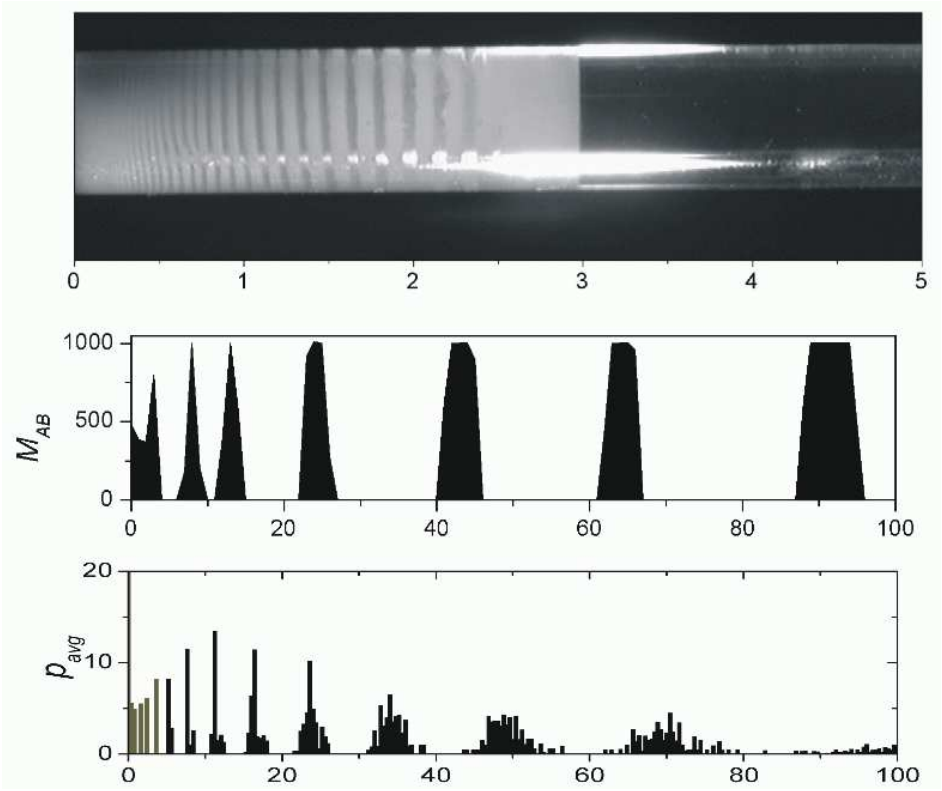


FIG. 2.1. *Precipitation patterns in the absence of an electric field. Experimental (top): the evolution time is 40.8 h, black strips represent the solid precipitate with length scale 1 cm. Spatial distribution of the precipitate in a single simulation of the discrete stochastic model (middle). Variation of the average amount of the precipitate ($P_{avg}$) in the diffusion column at $\tau = 5 \cdot 10^6$ (bottom) using the macro level stochastic model. The distribution of the precipitate corresponds to the average of 100 independent simulations. The first three bands correspond to the deterministic band positions. In the numerical simulations (middle, bottom) we applied a dimensionless length scale.*

Formation of precipitate stops wherever $M_P[i]$ reaches a maximal value $M_{P,\max}$. The reaction probability (the probability that a given particle $A$ transforms into precipitate) is given by $q_A[i](t) = \Delta[i](t)/\mathrm{SUM}_A[i](t)$ and similarly for particles $B$. In this way $1 - q_A[i](t)$ gives the probability that a particle $A$ (in the time interval $(t, t+h)$ in the $i$th segment) does not form to precipitate, only these can be recognized at time $t + h$ as existing particles $A$. If $j \le i \le k$ then the probability that a given particle $A$ or $B$, which moves from the $j$th segment to $k$th one, does not transform into precipitate is:

$$\prod_{j \le i \le k} 1 - q_A[i](t) \quad \text{and} \quad \prod_{j \le i \le k} 1 - q_B[i](t).$$

Therefore obtain for the modified transition probabilities:

$$p^*_\epsilon[j][k] = p_\epsilon[j][k] \prod_{j \le i \le k} 1 - q_A[i](t),$$

which yields the probability that a particle $A$ moves from the $j$th to $k$th segment and does not form to $P$ in the meantime (similarly to particles $B$). In the simulation procedure for particles $A$ in the $j$th segment we created discrete intervals in $[0,1]$ of length $p^*_\epsilon[j][1], p^*_\epsilon[j][2], \ldots, p^*_\epsilon[j][I]$ and for each of the particles a random number RND in $[0,1]$. If this fell into the interval corresponding to $p^*_\epsilon[j][k]$ then we pushed the particle into the $k$th segment. Anyway, if none of the intervals covered RND, it was transformed to $P$. We proceed similarly for particles $B$. Indeed, we have the transition probability matrices in a general sense [12] such that the sums of the rows and columns is at most *one*. For accelerating the computations we rather proceed with the above vector representation due to the sparse structure of the transition probability matrix.

**3. Results and discussion.** In Fig.2.1 one can see the Liesegang zones in a real experiment together with the results of the micro and the macro level simulations. The real experiments were carried out in a U tube (of diameter 0.5 cm and length 25 cm). The gel contained the inner electrolyte ($K_2Cr_2O_7$) with concentration 0.0036 M. The gel was contact with the solution of $K_2Cr_2O_7$ (0.0036 M) and $AgNO_3$ (outer electrolyte, 5 m/m %), respectively. Evolution of the Liesegang patterns were monitored by a computer controlled image system.

In case of the discrete stochastic simulation: $I = 300$, $K = 1400$, $L = 300$ and $M_{AB\max} = 1000$. These parameter values were chosen in accordance with of a formerly proposed deterministic model. We applied no-flux boundary conditions. Simulations were carried out till time step 60000. Initial values were $M_B[i](t = 0) = 100$, $M_{AB}[i](t = 0) = 0$ and $M_A[i](t = 0) = 0$, but $M_A[1](t) = 100$ at all times. Qualitatively we obtained similar precipitate distribution: high amount of the precipitate at the several regions and gaps without precipitate between them.

We also investigated the evolution of the pattern structure. Fig. 3.1 reflects the experimental and the numerical findings that the electric field modifies the mass transport characteristics of the electrolytes. Ionic migration flux of both electrolytes changes the spatiotemporal evolution of Liesegang patterns in the same way both in the real experiments and during the simulations.

In the absence of an electric field dependence of band position on the square root of its formation time is linear. This is a direct consequence of the diffusion process in our system. This dependence in the presence of an electric field can be given with a second-order polynomial (Fig. 3.2). Decreasing electric field strength, the spatial distribution of bands becomes more stochastic as shown in Fig. 3.2. We called a precipitate band position stochastic if after the averaging process this band occupies more than one spatial grid cell/segment. Otherwise it was considered deterministic. The high values of standard deviation (band position and its formation time) in the experiments can be recognized as a stochastic behavior of the reaction-diffusion system. In both simulations standard deviations are monotone increasing with the number of bands and the position.

Results of both models show that these approaches are successful for the description of regular Liesegang patterning in the presence and the absence of an electric field. We predicted that the stochastic precipitate pattern distribution depends on the electric field strength using a micro and a macro level approach. Liesegang patterns have been found to be increasingly deterministic, in terms of reproducibility of the band locations and of band formations as the electric field promotes the transport of the outer electrolytes.

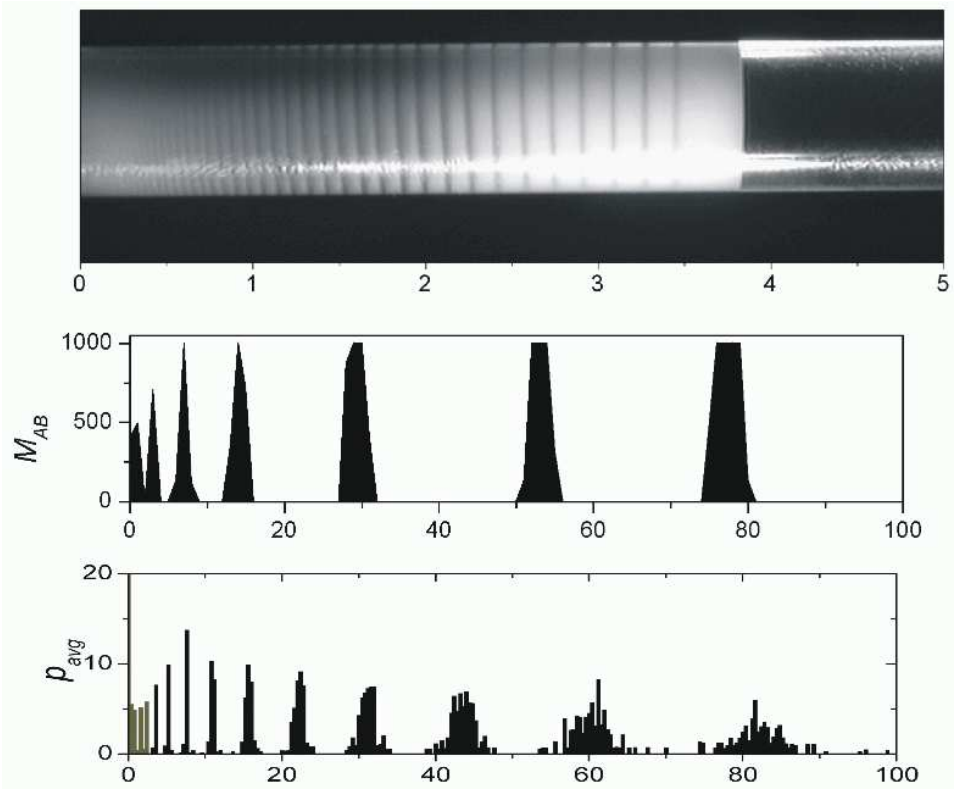


FIG. 3.1. *Precipitation patterns in the presence of an electric field. Experimental (top): the evolution time is also 40.8 h,* $E = 12Vm^{-1}$ *with length scale 1 cm. Spatial distribution of the precipitate in a single simulation of the discrete stochastic model for* $\epsilon_+ = 0.01$ *(middle). Variation of the average amount of the precipitate (*$P_{avg}$*) in the diffusion column at* $\tau = 5 \cdot 10^6$ *(bottom) using the macro level stochastic model. The distribution of the precipitate corresponds to the average of 100 independent simulations for* $\epsilon = 0.0025$*. The first two bands correspond to the deterministic band positions. In the numerical simulations (middle, bottom) we applied a dimensionless length scale.*

**Acknowledgments.** The authors thank Prof. Zoltán Rácz for his advice. We also acknowledge the support of the OTKA Postdoctoral Grant No. D048673 and OMFB grant 00585/2003 (IKTA5-137) of the Hungarian Ministry of Education.

REFERENCES

[1] R. E. LIESEGANG, *Über einige Eigenschaften von Gallerten*, Naturwiss. Wochenschr., 11 (1896), pp. 353–362.
[2] J. GEORGE AND G. VARGHESE, *Formation of periodic precipitation patterns: a moving boundary problem*, Chem. Phys. Lett., 362 (2002), pp. 8–12.
[3] T. ANTAL, M. DROZ, J. MAGNIN, Z. RÁCZ AND M. ZRÍNYI, *Derivation of the Matalon-Packter law for Liesegang patterns* , J. Chem. Phys., 109 (1998), pp. 9479–9486.
[4] M. DROZ, J. MAGNIN AND M. ZRÍNYI, *Liesegang patterns: Studies on the width law*, J. Chem. Phys., 110 (1999), pp. 9618–9622.
[5] S. KAI, S. C. MÜLLER AND J. ROSS, *Periodic precipitation patterns in the presence of concentration gradients 2. Spatial bifurcation of precipitation bands and stochastic pattern-formation*, J. Phys. Chem., 87 (1983), pp. 806–813.
[6] F. IZSÁK AND I. LAGZI, *Simulation of Liesegang pattern formation using a discrete stochastic*

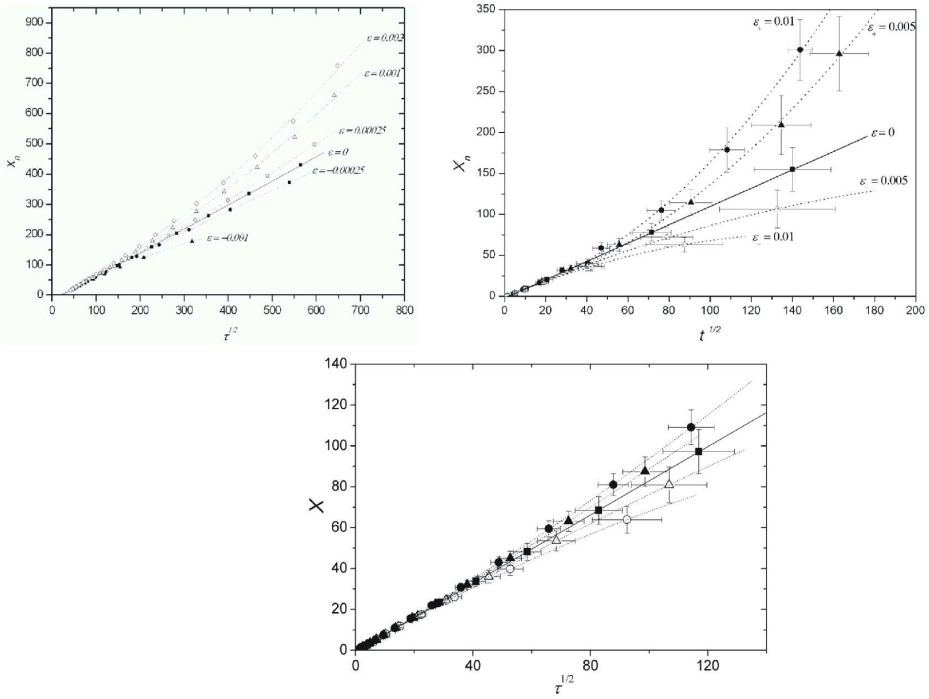


FIG. 3.2. *Dependence of the distance of bands (measured from the junction point of the two electrolytes) on the square root of its formation time (time law). Deterministic simulations (top, left), discrete stochastic simulations (top, right), and perturbed deterministic simulations (bottom). The error bar represents to the standard deviation of the spatial positions and square root of the corresponding formation time.*

*model*, Chem. Phys. Lett., 371 (2003), pp. 321–326.

[7] F. IZSÁK AND I. LAGZI, *Precipitate pattern formation in fluctuating media*, J. Chem. Phys., 120 (2004), pp. 1837–1840.

[8] A. BÜKI, É. KÁRPÁTI-SMIDRÓCZKI AND M. ZRÍNYI, *Computer-simulation of regular Liesegang structures*, J. Chem. Phys., 103 (1995), pp. 10387-10392.

[9] A. BÜKI, É. KÁRPÁTI-SMIDRÓCZKI AND M. ZRÍNYI, *2- dimensional chemical-pattern formation in gels - Experiments and computer-simulations*, Physica A, 220 (1995), pp. 357-375.

[10] W. OSTWALD, *Über die Geschwindigkeitsfunktion der Viskosität disperser Systeme*, Kolloid Z., 36 (1925), pp. 380.

[11] A. TAMIR, *Application of Markov Chains in Chemical Engineering*, Elsevier, Amsterdam, 1997.

[12] H. M. TAYLOR AND S. KARLIN, *An Introduction to Stochastic Modeling*, Third ed., Academic Press, New York, 1998.